



OPEN

A PBPK modeling approach for personalized dose optimization of nicardipine in renal and hepatic dysfunction

Ammara Ayub¹, Ammara Zamir¹, Muhammad Fawad Rasool^{1✉}, Usman Arshad² & Faleh Alqahtani^{3,4✉}

Nicardipine is a calcium channel blocker employed to manage hypertension and angina. It is primarily metabolized in the liver; therefore, hepatic impairment patients may experience drug accumulation, potentially resulting in adverse events. This research aims to design physiologically based pharmacokinetic (PBPK) model capable of accurately predicting the exposure of nicardipine in healthy individuals as well as hepatic and renal impairment patients. An extensive literature review was conducted to retrieve relevant articles and pharmacokinetic (PK) parameters of nicardipine, for integration into the PK-Sim[®] program. The modeling approach incepts with the development of healthy PBPK model, which is subsequently extrapolated to diseased populations to assess the alignment of anticipated and reported concentration-time profiles. The precision of the model was then evaluated through visual predictive checks, mean observed–predicted ratios, and average fold error across relevant PK parameters, which adhered to the predefined 2-fold threshold. The observed exposure of nicardipine in Child-Pugh A was found to be ~1.5-fold greater than in a healthy population, highlighting the necessity of dosage adjustment in the cirrhotic population. The developed PBPK models have effectively elucidated the PK alterations of nicardipine in healthy and diseased populations, thus the insights gained from these models can inform tailored dosing regimens for enhancing therapeutic efficacy.

Keywords Nicardipine, PBPK model, Hypertension, Liver cirrhosis, Renal impairment

Physiologically Based Pharmacokinetic (PBPK) models play a critical role in drug development by enabling predictions of biodistribution and toxicity of various pharmaceuticals^{1–4}. Originating from Teorell's 1937 concept, PBPK modeling was first applied in clinical research in 1977 using preclinical in vitro data^{5,6}. PBPK models differ from compartmental models by simulating organ-specific compartments interconnected via physiological blood flow⁷. The integration of physiological, drug-related parameters, and the PK data in PBPK models facilitates the accurate prediction of drug disposition and dosage optimization^{8,9}. Numerous publications have emerged over the past several decades that examine the use of PBPK modeling in the context of various drugs^{10–15}.

Nicardipine is classified as a dihydropyridine-type calcium (Ca^{2+}) channel blocker. It is indicated for the management of hypertension, stable angina, and Prinzmetal's angina¹⁶. This drug acts by inhibiting long-acting Ca^{2+} channels, thereby inducing vasorelaxation^{17–19}. The Biopharmaceutics Classification System (BCS) categorizes this drug as a class II drug, indicating elevated permeability and poor aqueous solubility of 7.9 mg/mL²⁰. It exhibits a complex metabolism predominantly mediated by the cytochrome P450 (CYP) enzyme system, with CYP3A4 serving as the major contributor and CYP2C8 and CYP2D6 contributing to a lesser extent, influencing its PK profile²¹. Following oral administration, it undergoes rapid absorption but undergoes a substantial first-pass effect, reducing its bioavailability to ~35%^{22,23}. The resulting metabolites, including, pyridine analogue metabolites (M-5)^{24,25}, are excreted via urine (~40%) and bile (60%)²⁶, and its hepatic clearance (CL_H) in healthy populations is reported to be $58.68 \pm 13.32 \text{ L/h}$ ²⁷.

¹Department of Pharmacy Practice, Faculty of Pharmacy, Bahauddin Zakariya University, 60800 Multan, Pakistan. ²Clinical Pharmacology Modeling and Simulation, GSK, Gunnels Wood Road, Stevenage SG12NFX, UK. ³Department of Pharmacology and Toxicology, College of Pharmacy, King Saud University, Riyadh 11451, Saudi Arabia. ⁴King Salman Center for Disability Research, Riyadh 11614, Saudi Arabia. ✉email: fawadrasool@bzu.edu.pk; afaleh@ksu.edu.sa

Various pathophysiological changes are observed in LC and CKD that can influence several physiological parameters, including blood flow to all organs, hematocrit levels, liver volume fraction, plasma protein scale factor, estimated glomerular filtration rate (eGFR), small intestinal transit time, etc. which have been documented in previously published clinical research studies^{28–31}. Notably, the PK of nicardipine may be altered in patients with LC and CKD, leading to increased drug exposure. Consequently, the integration of these physiological variations into a drug-disease PBPK model may enhance the accuracy of predictions regarding the drug's disposition thus facilitating optimal dosing strategies for patients with these medical conditions.

Currently, there is only one reported application of the PBPK model for nicardipine, which has specifically examined CYP3A4-mediated drug interactions between saxagliptin and nicardipine³². The current investigation endeavors to develop and evaluate a PBPK model capable of anticipating the ADME of nicardipine in healthy individuals, as well as in patients with CKD and LC, by employing a systematic modeling framework. The purpose of this study is to develop and evaluate drug-disease PBPK models for nicardipine following the incorporation of pertinent pathophysiological changes associated with CKD and LC to recommend appropriate dosage modifications in such patients, thus ensuring optimal therapeutic efficacy and safety.

Methodology
Pharmacokinetic studies screening

A comprehensive search was conducted across various databases, including Google Scholar, PubMed, ScienceDirect, and the Cochrane Library, to gather relevant articles pertaining to the PK of nicardipine. The screening was concentrated on administering nicardipine through both IV and oral routes, particularly emphasizing the plasma concentration–time profiles observed in healthy and diseased populations. The analysis comprised a total of 10 studies, encompassing 6 profiles related to IV dosage form, 7 profiles pertaining to oral administration in healthy individuals, two profiles focused on patients with CKD, and one profile involving LC subjects. The development and evaluation process of PBPK modeling employed one-third (2 for each IV and oral) and two-thirds (4 for each IV and oral) studies, correspondingly. The demographic parameters of all the included studies are outlined in Table 1.

Software employed for PBPK model

For the development of the PBPK model and assessment of the ADME of nicardipine in healthy and diseased (CKD and LC) populations, the whole-body simulation software i.e. PK-Sim version 11.3, developed by Bayer Technology Services GmbH Systems Biology Software Suite Wuppertal, Germany⁴³ (available at <https://github.com/Open-Systems-Pharmacology>), was employed. The Get Data Graph Digitizer software (Version 2.24.0) was employed to extract quantitative data from graphs in the included articles.

Building blocks development

PK-Sim software features a user-centered graphical interface with distinct building blocks, enabling efficient operations and comprehensive simulation features. The drug-specific and physiological parameters, as well as PK data of nicardipine based on established values derived from relevant clinical studies in healthy, CKD, and LC

Dosage	Study size	Gender	F Prop. (%)	Age (years)	References
Intravenous administration in healthy population					
0.16 mg/kg	14	M	0	21–40	33
5 mg/h ^a	6	M	0	NN	34
0.885 mg	6	M	0	24–33	35
1.05 mg	1	F	100	32	36
5 mg	8	M and F	50	51 ± 9	37
210 ug/kg ^b	8	M	0	19–28	38
Oral administration in healthy population					
30 mg	6	M	0	NN	34
40 mg	1	F	100	32	36
30 mg	8	M	0	30–63	39
20 mg	8	M and F	37.5	23–45	40
30 mg	9	M and F	11.1	21–42	41
20 mg	NN	NN	NN	NN	42
Oral administration in mild cirrhotic patients					
30 mg	9	M	0	31–66	39
Oral administration in chronic kidney disease					
20 mg ^c	12	M and F	33.3	19–75	41
30 mg ^d	9	M and F	11.1	18–69	41

Table 1. Summary of clinical studies employed in the development of Nicardipine PBPK model. *M* male, *F* female, *Prop* proportion, *NN* not narrated. ^aDose infused over 3 h, ^bdose infused over 30 min, ^cmoderate renal failure, ^dsevere renal impairment.

populations, were embedded into PK-Sim software for PBPK model configuration, as demonstrated in Table 2 and Supplementary Tables ST2 and ST3. PK-Sim provides three built-in cellular permeability models: PK-Sim Standard, Charge Dependent Schmitt, and Charge Dependent Schmitt normalized to PK-Sim. In this study, simulations were conducted using the PK-Sim Standard model, calculating permeability parameters from the physico-chemical parameters given in the compound data window. The degree of dissociation of acids and bases is not taken into account. It is assumed that this value is the same in all organs and that differences originate only from size-dependent surface areas.

Strategic approach for model development

The development of the PBPK model was initiated by conducting an exhaustive literature search for the screening of relevant PK parameters and plasma concentration-time profiles for nicardipine. Subsequently, for the purpose of validating the model in healthy individuals, drug-specific parameters, system-related parameters, and PK profiles were integrated into PK-Sim, developing IV and oral models based on previously recognized modeling techniques^{10,11,14,51–53}. The sensitivity analysis was performed for model parameters: fraction unbound (f_u), lipophilicity (log P), specific intestinal permeability, and hepatic clearance (CL_H) as shown in the supplementary document (Figure SF1 and Table ST1). The IV model was established first, subsequently leading to the creation of the oral model, which was designed without altering the existing parameters. This approach was taken to mitigate the complexities associated with absorption parameters, particularly those related to specific intestinal permeability. To enhance the model's relevance for diseased states, particularly those with LC and CKD, different pathophysiological alterations were systematically integrated into the PBPK model. The mathematical equations employed for PBPK model development are documented in the Supplementary Table ST4. The classification of organs into slowly perfused and highly perfused compartments was carried out automatically by the PK-Sim[®] software, utilizing its built-in physiological parameters. The diagram illustrating the organs involved in the PBPK model of drug and visual representation of this model framework are displayed in the Fig. 1A, B.

Model framework

Nicardipine is represented with molecular formula $C_{26}H_{29}N_2O_6$ ⁵⁴, and possesses a fraction unbound (f_u) of 0.0024–0.016^{49,50}. Moreover, it has a basic nature with a dissociation constant (pK_a) of 8.10⁵⁵. The model's prediction was guided by the Rodgers and Rowland model for cellular permeability and the standard partition coefficient model of PK-Sim. The formulation parameters were optimized by utilizing the Weibull model. For the tablet, sustained-release (SR) capsules, and oral solution, the specified dissolution times (50% dissolved) were 10, 15, and 0.5 min, respectively. Furthermore, the dissolution shape values were designated as 2 for the tablet, 0.2 for the SR capsule, and 1 for the oral solution after performing visual predictive checks (VPC). The additional parameters used in developing the model are presented in the Table 2.

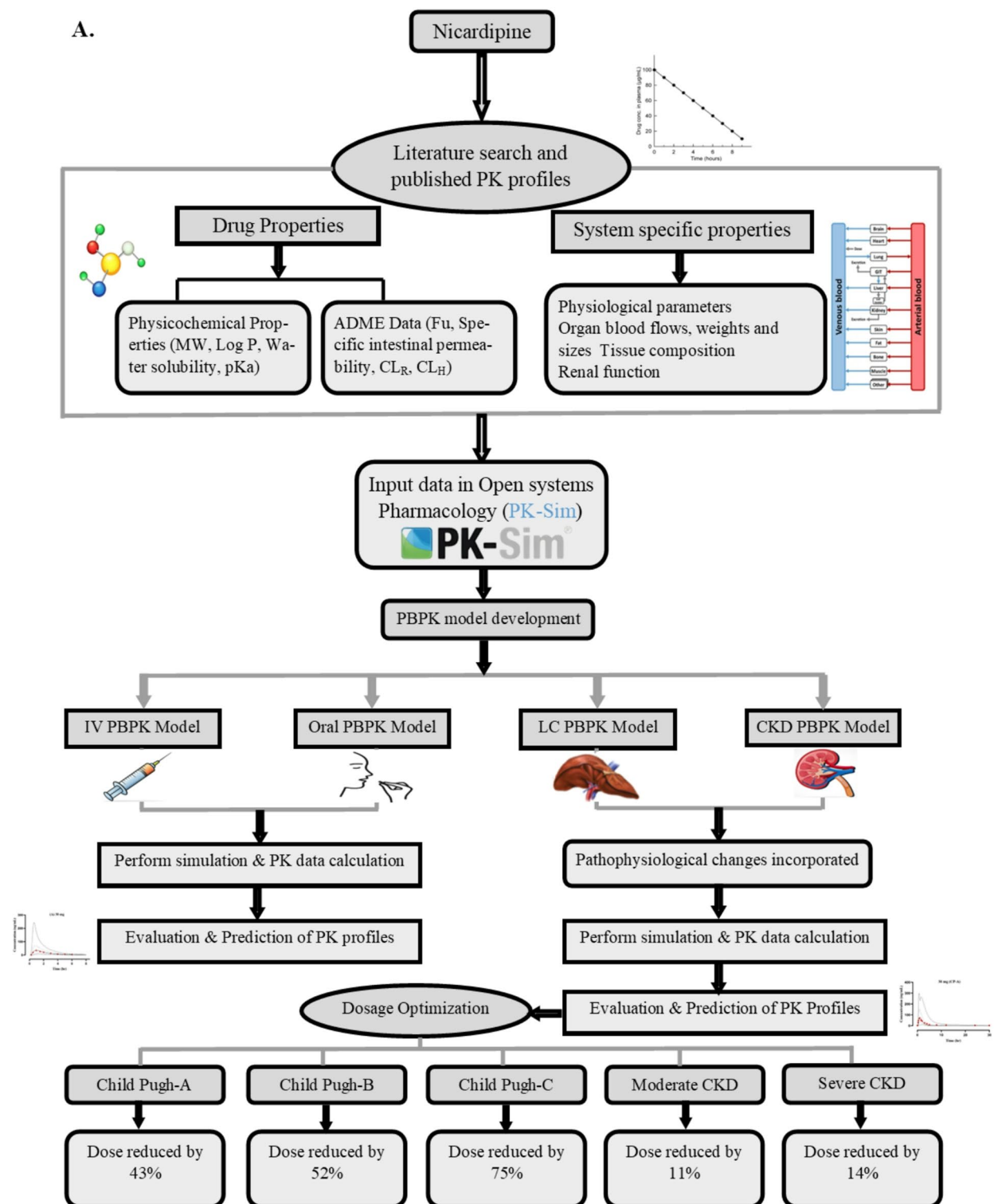
PBPK model for diseased population

Chronic kidney dysfunction

CKD is characterized by a reduction in renal function that persists for at least three months, indicated by a glomerular filtration rate (GFR) of less than 60 mL/min per 1.73 m²⁵⁶. Various pathophysiological alterations occur in CKD, such as alterations in levels of plasma protein (specifically albumin), hematocrit, small intestinal transit time, and gastric emptying time^{30,31}, which subsequently alters the ADME of nicardipine. In the profiles of moderate and severe CKD, the estimated glomerular filtration rates (eGFR) were incorporated into model

Parameters	Incorporated value	References
Physicochemical characteristics		
Molecular wt. (g/mol)	479.5	44
pK_a	8.1	45
Plasma protein binding	Albumin	46
Water solubility at pH 7 (mg/ml)	7.9	20
Log P (log units)	3.5	47
Absorption		
Intestinal permeability (specific) (cm/s)	7.60×10^{-6}	48
Distribution		
Cellular permeability model	PK Sim Standard	
Partition coefficient model	Rodgers and Rowland	
Specific organ permeability (cm/min)	0.3	Optimized
Unbound drug fraction (f_u)	0.004	49,50
Disposition (metabolism and elimination)		
Hepatic clearance (mL/min/kg)	11.8 ^a	27
Renal clearance (mL/min/kg)	4 ^b	27

Table 2. Input variables for nicardipine model development. *Log P* lipophilicity, pK_a acid-dissociation constant. ^aThe model employs a value of 0.71, expressed in L/h/kg. ^bThe model employs a value of 0.24, expressed in L/h/kg.



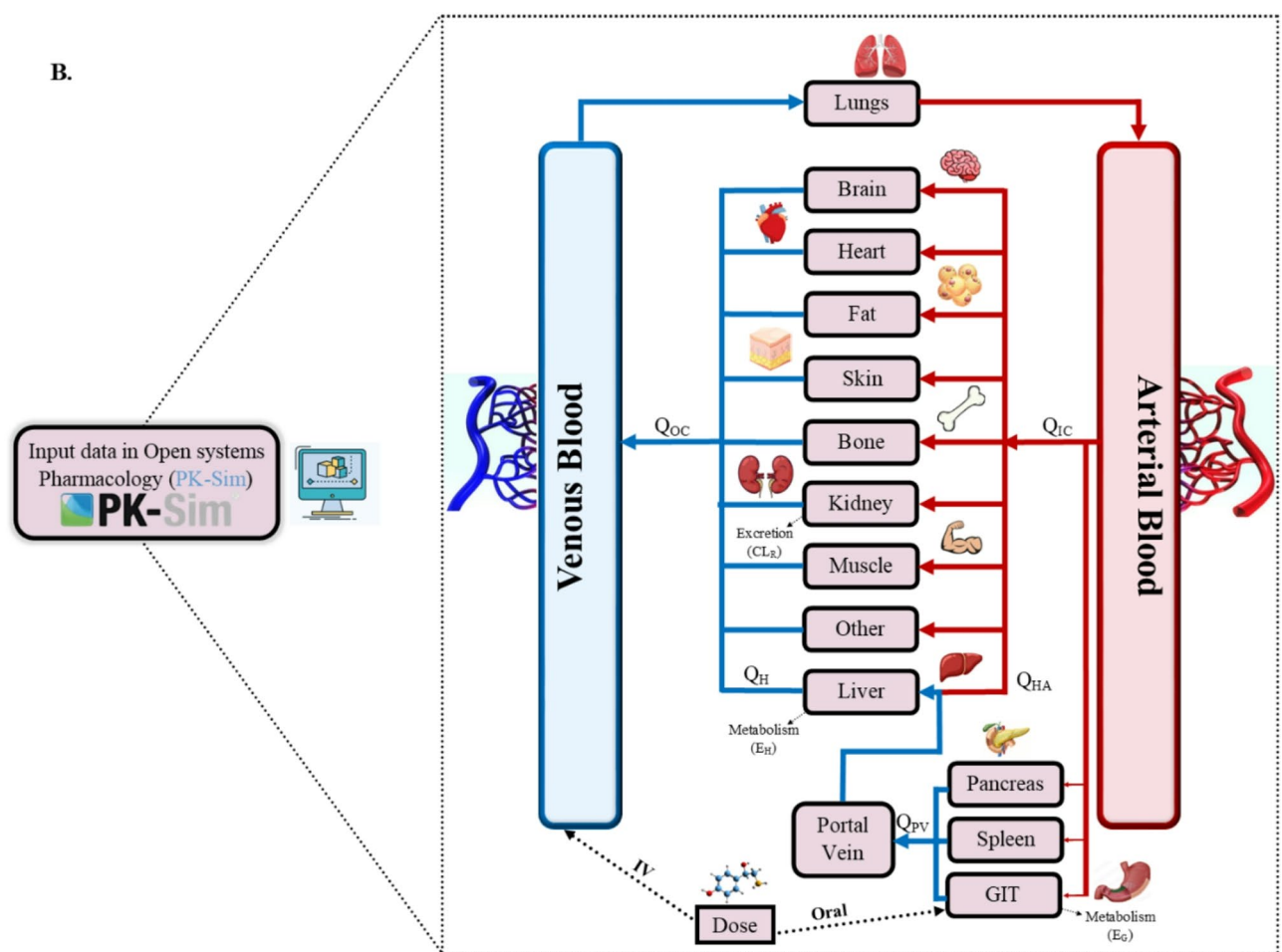


Fig. 1. (continued)

as 35.01 and 26 mL/min/1.73 m², respectively. Other in-built pathophysiological changes for various stages of CKD were integrated into the PK-Sim virtual populations to refine the drug-disease model. The $AUC_{0-\infty}$ was analyzed and compared among three distinct populations: healthy, moderate CKD, and severe CKD, followed by a rigorous evaluation of the model through comparison with the reported profiles. Furthermore, box-whisker plots were deployed to visually illustrate the data, providing dosage recommendations for nicardipine.

Liver cirrhosis

LC is a progressive condition characterized by a decline in liver function, accompanied by significant morphological and pathophysiological alterations. The progression of this disease is typically classified according to the Child-Pugh (CP) grading system, which includes three categories; mild (CP-A), moderate (CP-B), and severe (CP-C)⁵⁷. A PBPK model for cirrhotic patients was developed, based on pathophysiological changes in the functional size of the liver, expression of CYP450, GFR, cardiac output, hematocrit, hepatic blood flow, as well as plasma albumin concentrations, as detailed in Table 3^{57,58}. These changes may influence the systematic exposure of nicardipine administered to the patient, making it imperative to evaluate drug PK to assess potential risks and investigate any alterations in ADME of the drug under cirrhotic conditions. The study selected for the verification of the nicardipine PBPK model in LC presented a plasma concentration versus time curve for a population classified as CP-A³⁹, the predictions of which were visually validated through the comparison of reported data and the anticipated data. Moreover, Box whisker plots were employed to visually illustrate the results of dose optimization.

Model evaluation and verification

All the PK profiles were evaluated using a simulated cohort of 1,000 individuals, designed to reflect the characteristics of clinical studies, including demographic and physiological variables such as age, gender, and body weight, as well as dosage and administration routes. A subsequent evaluation of the nicardipine model was conducted by utilizing VPC to verify the robustness of the model. This technique involves evaluating PK models by visual comparison of anticipated data against reported data. By plotting these datasets over time or across various parameters, researchers can effectively assess how well the model captures the fluctuations and trends present in the observed data⁵⁹. The assessment of the model was conducted by the comparison of

Variables	Control	PK-Sim default	CP-A
Functional liver volume ^a	1	2.2	0.81
Hematocrit (%) ^a	40.9	0.47	36.6
Plasma protein factor ^b	–	1	0.81
GFR (mL/min) ^a	120	21.5	83.7
Blood flow (mL/min) ^b			
Liver	–	18.83	1.3
Kidney	–	228.58	0.88
Bone and other organs	–	–	1.75

Table 3. Pathophysiological alterations observed in liver cirrhosis. ^aReference values extracted from²⁹, ^bReference values extracted from²⁸.

the predicted arithmetic mean, the 5th to 95th percentiles, as well as the minimum and maximum plasma concentrations against the mean plasma concentration vs. time curves obtained from the reported clinical data. The PK parameters were calculated by employing non-compartmental analysis (NCA) in the PK-Solver^{*}, an add-in program, Version 2016⁶⁰. In studies conducted on healthy subjects, the mean predicted-to-observed ($R_{pre/obs}$) ratios for clearance (CL), C_{max} , and $AUC_{0-\infty}$ were computed utilizing Eq. (1), with a 95% confidence interval. In contrast, for diseased (CKD and LC) subjects, data were expressed as mean and range, owing to the availability of limited studies. These ratios, as predicted by the previously published PBPK models, are expected to fall within a two-fold range^{10,11,14,51–53}. To determine $R_{pre/obs}$, average fold error (AFE), and fold error, the following Eqs. (1)–(3) are employed, as provided below:

$$R = \frac{\text{Predicted value of PK parameter}}{\text{Observed value of PK parameter}} \quad (1)$$

$$\text{Fold - error} = \frac{\text{Predicted values of parameter}}{\text{Observed values of parameter}} \quad (2)$$

$$AFE = 10^{\frac{\sum \log(\text{fold error})}{N}} \quad (3)$$

Results

The systematic methodology employed to achieve the results is presented in Fig. 1.

Designing and evaluating PBPK model for healthy subjects

The PBPK model anticipated plasma concentration-time data for nicardipine were contrasted with the reported PK data following the IV (bolus and infusion) and oral doses. The predictive accuracy for the concentration-time profile was confirmed, as the reported data fitted well within the 5th – 95th percentile and was comparable with the predicted arithmetic mean as displayed in Figs. 2 and 3. The accuracy of the nicardipine model was further supported by calculating the average fold error (AFE) value, which reflected the average deviation between the reported and anticipated values, displaying the maximal plasma concentration (C_{max}) of 0.875 and 1.14 upon IV and oral administration (Table 5). Moreover, $R_{pre/obs}$ ratios of other PK variables i.e. CL and area underneath the curve from time zero to infinity ($AUC_{0-\infty}$), were consistent and adhered to the predefined 2-fold threshold (Table 4; Fig. 4).

Development and evaluation of the PBPK model in population with LC and CKD population

In patients with CKD and LC, the reported data aligned well with the anticipated concentration-time profiles of nicardipine. This alignment was observable for both the arithmetic mean and the 5th to 95th percentile, as illustrated in Figs. 5 and 6. Moreover, these results were validated by the AFE values, which reported the (C_{max}) for CKD and LC individuals as 0.664 and 1.17, respectively (Table 5), and the $R_{pre/obs}$ ratios for each relevant PK parameter, which adhered to the permissible two-fold error threshold, are displayed in Fig. 4; Table 5.

Dosage modification of Nicardipine in LC and CKD patients

Following the oral administration of similar doses of nicardipine, the patients with LC displayed significantly higher $AUC_{0-\infty}$ than healthy individuals. A dosage adjustment method was implemented gradually through careful tapering and simulations to attain comparable nicardipine exposure among healthy subjects and LC patients. The exposure levels of the drug were rendered equivalent by reducing the dose by 75% of the original 30 mg dose in the case of the CP-C population as evidenced in the box-whisker plot shown in Fig. 7. In contrast, the dosage of nicardipine was reduced by 43% and 52% in the case of individuals with CP-A and CP-B, correspondingly. However, in patients with moderate to severe CKD, the dosage of nicardipine was adjusted, being reduced by 11% and 14% from the initial dose of 30 mg, respectively, to maintain comparable exposure levels. This approach of dosage optimization adhered to the methodologies detailed in previously published studies⁶¹. The box-whisker plots (Figs. 7 and 8) illustrating the simulated exposure of oral nicardipine administration in healthy population, LC, and CKD subjects highlight the process of dose optimization.

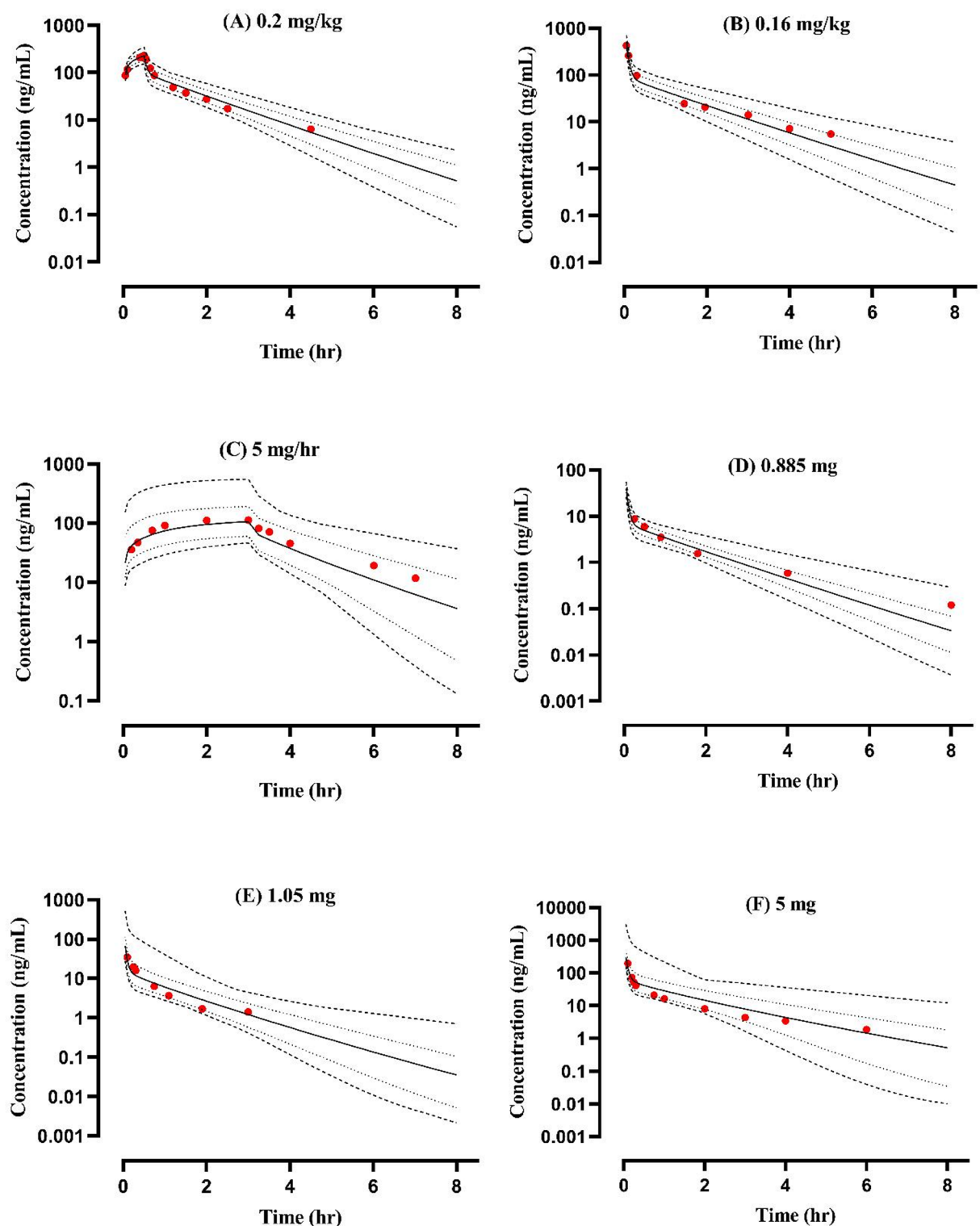


Fig. 2. The contrast of reported and anticipated systemic concentration vs. time profiles of nicardipine following Intravenous doses of; (A) 210 $\mu\text{g/kg}$ for 30 mins³⁸, (B) 0.16 mg/kg ³³, (C) Infusion of 5 mg/h over 3 hr³⁴, (D) 0.885 mg ³⁵, (E) 1.05 mg ³⁶, (F) 5 mg ³⁷, respectively. (Red dots): Values of observed data, (straight line): Arithmetic mean prediction, (dashed line): dashed lines-maximum and minimum values, (black dotted line): dotted lines-5th and 95th percentile.

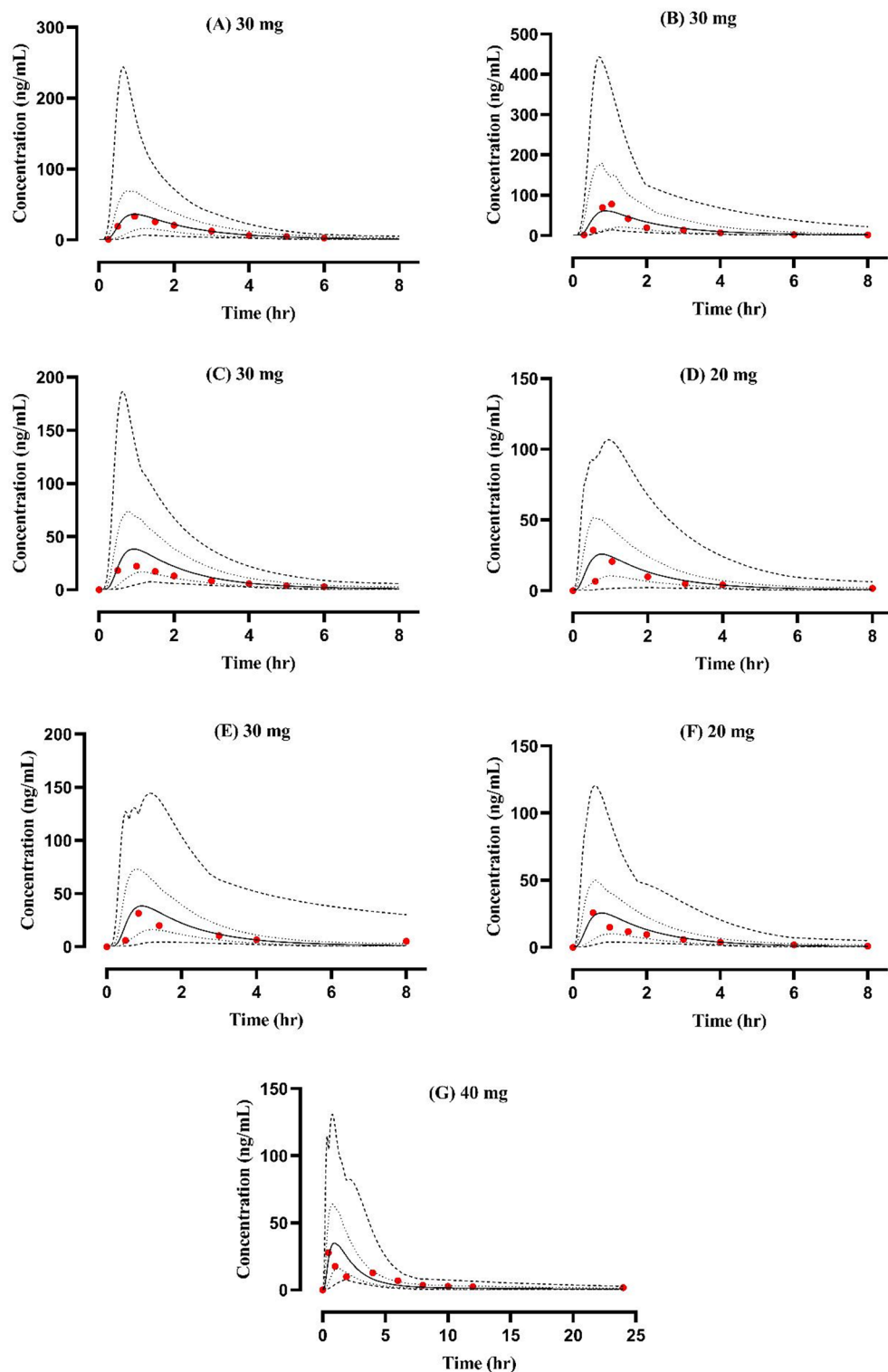


Fig. 3. The contrast of reported and anticipated systemic concentration vs. time profiles of nicardipine following oral doses (in mg) of; (A) 30 mg³⁴, (B) 30 mg³⁶, (C) 30 mg⁴⁰, (D) 20 mg⁴¹, (E) 30 mg⁴¹, (F) 20 mg⁴², (G) 40 mg³⁹, respectively. (Red dots): Values of observed data, (straight line): Arithmetic mean prediction, (dashed line): dashed lines-maximum and minimum values, (dotted line): dotted lines-5th and 95th percentile.

Dose	C _{max} (ng/mL)			AUC _{0-∞} (ng/mL.hr)			CL (L/h)			References
	O.V.	P.V.	R Ratio	O.V.	P.V.	R Ratio	O.V.	P.V.	R Ratio	
IV administration in healthy individuals										
210 ug/kg for 30 min	230.14	226.37	0.984	220.4	227.17	1.031	66.7	64.45	0.966	38
0.16 mg/kg	424.69	511.05	1.203	217.84	203.58	0.934	51.41	55.01	1.07	33
5 mg/hr for 3 h	123.3	105.44	0.855	447.32	360.76	0.806	33.53	41.58	1.24	34
0.885 mg	8.69	6.65	0.765	12.62	11.27	0.893	70.13	78.56	1.12	35
1.05 mg	34.65	29.25	0.844	21.08	21.58	1.023	49.8	48.66	0.977	36
5 mg	194.79	140.65	0.722	109.96	112.26	1.021	45.47	44.54	0.979	37
Oral administration in healthy individuals										
30 mg	78.09	60.52	0.775	116.98	142.16	1.215	256.46	211.03	0.823	34
40 mg	27.65	34.73	1.256	179.38	131.32	0.732	222.99	304.6	1.366	36
30 mg	33.27	36.26	1.089	83.06	85.95	1.035	361.17	349.74	0.968	39
30 mg	22.14	38.13	1.722	66.11	87.85	1.329	453.79	341.45	0.752	40
20 mg	20.63	24.35	1.18	52.92	62.99	1.19	393.88	317.47	0.806	41
30 mg	31.48	37.95	1.206	101.03	97.53	0.965	296.95	307.6	1.036	41
20 mg	25.82	24.29	0.941	52.03	60.4	1.161	384.35	331.1	0.861	42
Oral administration in CKD population										
20 mg	33.04	27.25	0.825	86.09	75.19	0.872	232.22	266	1.15	41
30 mg	55.02	31.86	0.579	152.02	103.50	0.680	194.45	290.44	1.494	41
Oral administration in LC population										
30 mg	67.12	74.45	1.109	307.21	173	0.563	97.65	173.41	1.775	39

Table 4. The $R_{pred/obs}$ ratios for PK parameters of Nicardipine in healthy and diseased populations. C_{max} maximal plasma concentration, $AUC_{0-∞}$ area underneath the curve from time zero to infinity, CL clearance, CKD chronic kidney disease, LC liver cirrhosis, IV intravenous, $O.V.$ the observed parameter value, $P.V.$ the predicted parameter value, $R\ Ratio\ P.V./O.V.$

Discussion

This investigation involves employing a systematic framework for constructing a detailed and comprehensive PBPK model for nicardipine, capturing the PK characteristics of the drug, analyzed after administering both oral and IV doses in healthy individuals as well as diseased populations (CKD and LC). Saturable first-pass metabolism is a notable characteristic of nicardipine pharmacokinetics, leading to complexities in drug absorption and bioavailability profiles. When administered orally, nicardipine undergoes significant first-pass metabolism in the liver and intestine, primarily mediated by cytochrome P450 enzymes, particularly CYP3A4. This metabolism results in a limited bioavailability of about 35% after oral dosing²³. Due to these metabolic pathways, some patients experience multiple plasma concentration peaks, a phenomenon attributed to variable intestinal absorption and hepatic clearance mechanisms⁶². The preliminary evaluations were performed in a healthy population before expanding the assessments to individuals diagnosed with certain diseased conditions, following the methodology established by previously published models^{10,11,14,51–53}.

In the present study, the PBPK model was created and evaluated by utilizing PK-Sim® software, enabling researchers to gain comprehensive insights into the PK behavior and elimination pathways of nicardipine. This model is constructed using the documented physicochemical characteristics and concentration vs. time profiles of the drug as reported in the studies for IV and oral dosing in healthy individuals, employing in silico methodologies. The results indicate that the predicted and observed values exhibited a strong correlation, as evidenced by the mean $AUC_{0-∞}$ values of 173.03 vs. 170.93 ng.hr/mL following IV dosage in healthy subjects. Furthermore, the mean predicted and observed $AUC_{0-∞}$ aligned closely i.e. 93.1 and 92.77 ng.hr/mL, respectively, and the calculated mean $R_{pre/obs}$ ratio for C_{max} in the healthy subjects was 1.02, which demonstrates the model's robustness to reliably forecast the PK of nicardipine. Moreover, the assessment of the AFE value for CL, following the oral administration of nicardipine, yielded a value of 0.95, which remained within the acceptable two-fold error range. This finding indicates that the model successfully reflects ADME processes for nicardipine through the utilization of precise and reliable input parameters.

Nicardipine is predominantly metabolized by the liver³⁴, indicating that its ADME may be significantly influenced by hepatic impairment. In individuals suffering from LC, variability in several parameters such as blood flow to various organs, GFR, plasma protein scale factor, liver volume fraction, and hematocrit, is frequently noted, which may significantly elevate the risk of developing irreversible complications^{28,29,63}. Furthermore, the Child-Pugh (CP) classification serves as a valuable tool for evaluating the extent of liver impairment. It is important to comprehend how these alterations may affect the PK of medications, which could ultimately result in adverse effects or reduced therapeutic effectiveness. The data obtained from simulations and actual measurements demonstrated that the $AUC_{0-∞}$ for nicardipine significantly increased by ~2.7 folds following oral administration in mild cirrhotic patients. The findings indicate that LC plays a significant role in causing pathophysiological changes by elevating drug exposure and plasma concentration levels while reducing

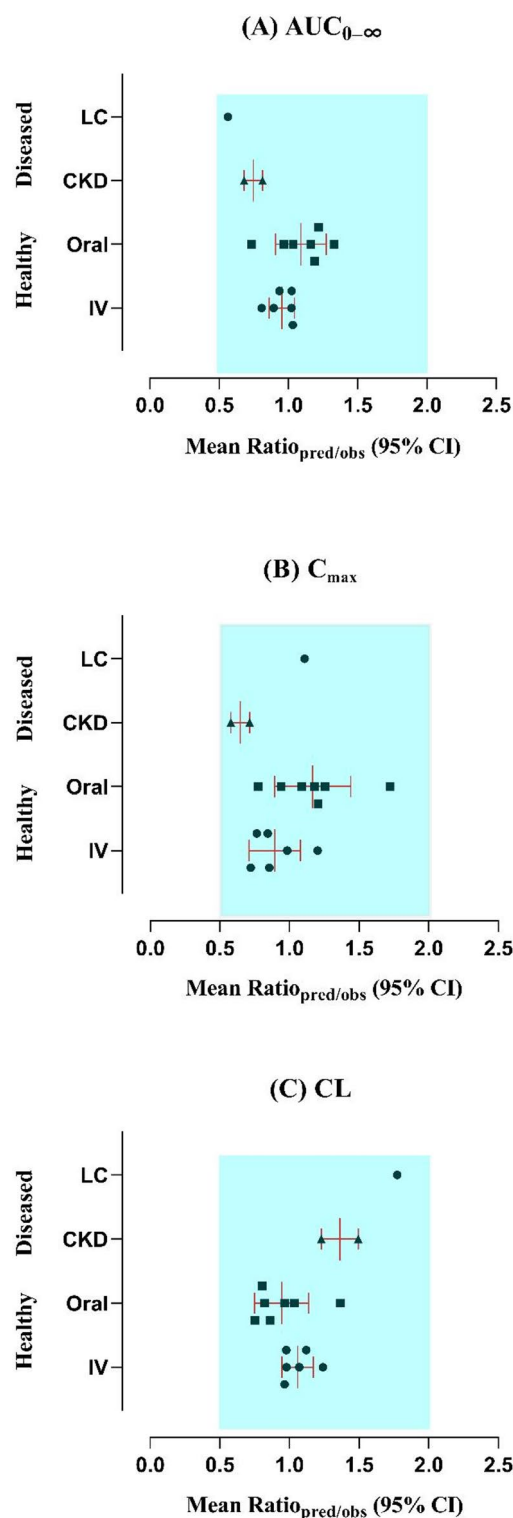


Fig. 4. The contrast of mean ($R_{\text{pred/obs}}$) ratios for the (A) area underneath the curve from time zero to infinity ($AUC_{0-\infty}$), (B) Maximal plasma concentration (C_{max}), and (C) Clearance (CL) amongst healthy individuals, and chronic kidney disease (CKD) and liver cirrhosis (LC) patients. The findings are reported alongside a 95% confidence interval (CI).

the CL. The evaluation of LC profiles involved a comparative assessment of $AUC_{0-\infty}$, which demonstrated that a dose reduction of 43%, 52%, and 75% is warranted for individuals classified as CP-A, CP-B, and CP-C patients, correspondingly. The suggested nifedipine dosage guidelines may provide valuable insight for managing LC in patients, potentially reducing the likelihood of further complications associated with their condition.

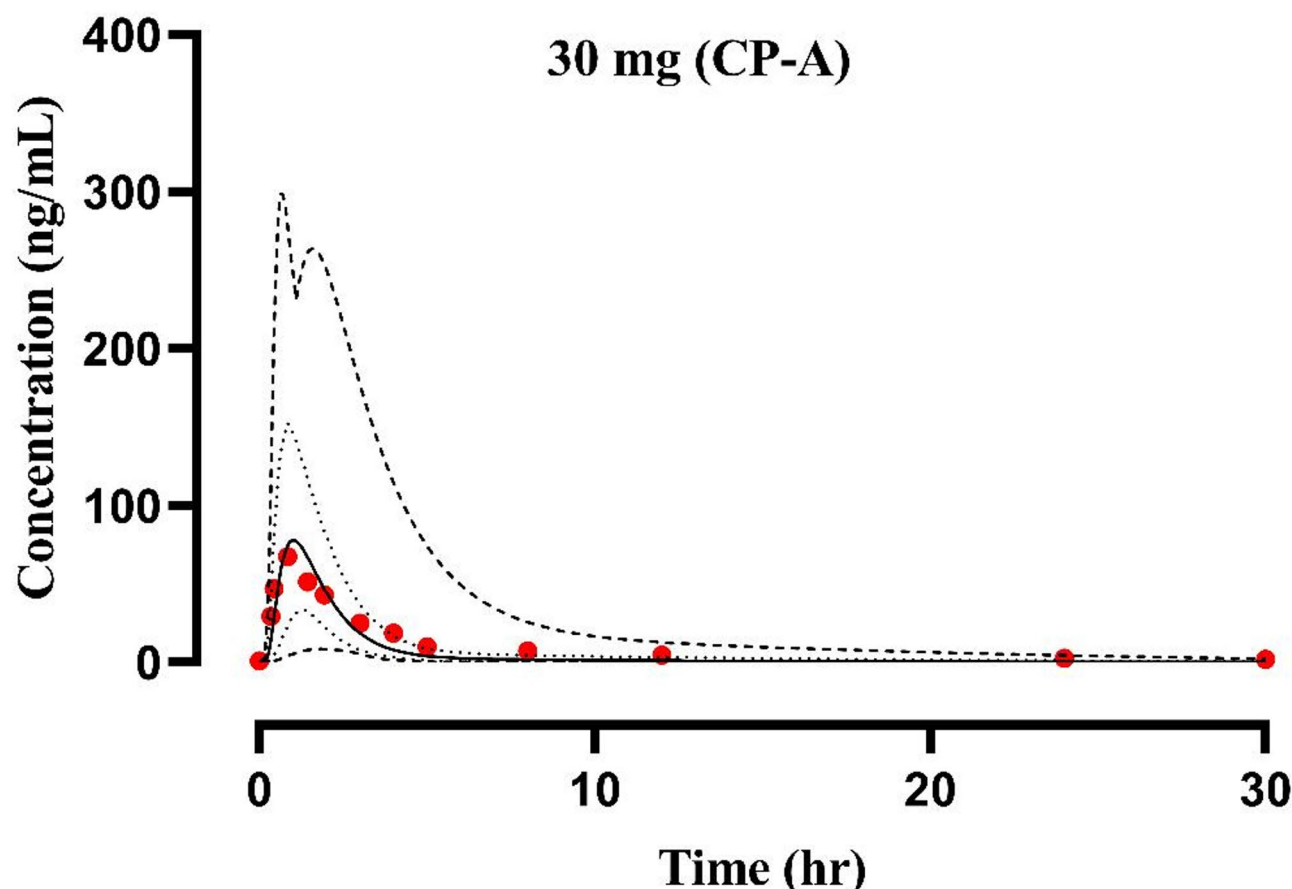


Fig. 5. The contrast of predicted and observed concentration vs. time curves following oral administration of 30 mg³⁹ nicardipine in mild liver cirrhotic (CP-A) patients. (Red dots): Values of observed data, (straight line): Arithmetic mean prediction, (dashed line): dashed lines-maximum and minimum values, (dotted line): dotted lines-5th and 95th percentile.

Numerous investigations have revealed that impaired renal function may lead to alterations in key physiological parameters, including GFR, small intestinal transit time, gastric emptying time, hematocrit, albumin, etc^{30,31,63,64}. Nicardipine is excreted from the body through the kidneys²⁵; therefore, its PK profile may be adversely affected in renal impairment patients. In CKD subjects, both simulation and observed data demonstrate a notable increase in the $AUC_{0-\infty}$ for nicardipine, with observed exposure increasing by 50–70% for moderate and severe CKD, and this observation aligns with the outcomes reported in earlier research studies³⁰. These results imply that CKD plays a crucial role in altering pathophysiological mechanisms, as it leads to a reduction in CL and an increase in plasma concentration levels, half-life, and bioavailability of the drug. Therefore, it is advisable to consider dosage adjustments in this population, as recommended in previously published studies²⁵. An assessment of CKD studies comparing $AUC_{0-\infty}$ revealed that patients with severe CKD require a dose reduction of 14%, whereas those with moderate CKD require a dose lowered by ~11%. The proposed dosage recommendations of nicardipine for CKD patients may help in managing their condition and alleviate the risk of disease progression.

Limitations

The systemic concentration of nicardipine over time obtained from publication graphs was carefully scanned for model evaluation. While the extracted PK parameters aligned closely with the reported values, minor discrepancies should not be neglected. Another notable limitation is that some studies used in the evaluation of the model lacked data on gender distribution. The available clinical PK data for nicardipine is predominantly sourced from studies following the oral administration of the drug in healthy subjects, cirrhotic, and renal impairment patients. Therefore, the predictions made by the model regarding IV administration for disease-afflicted populations cannot be supported. Future research could address this gap if pertinent IV studies in affected populations become available. Additionally, to substantiate the validity of the proposed model, there is a requirement for further clinical data pertaining to mild CKD.

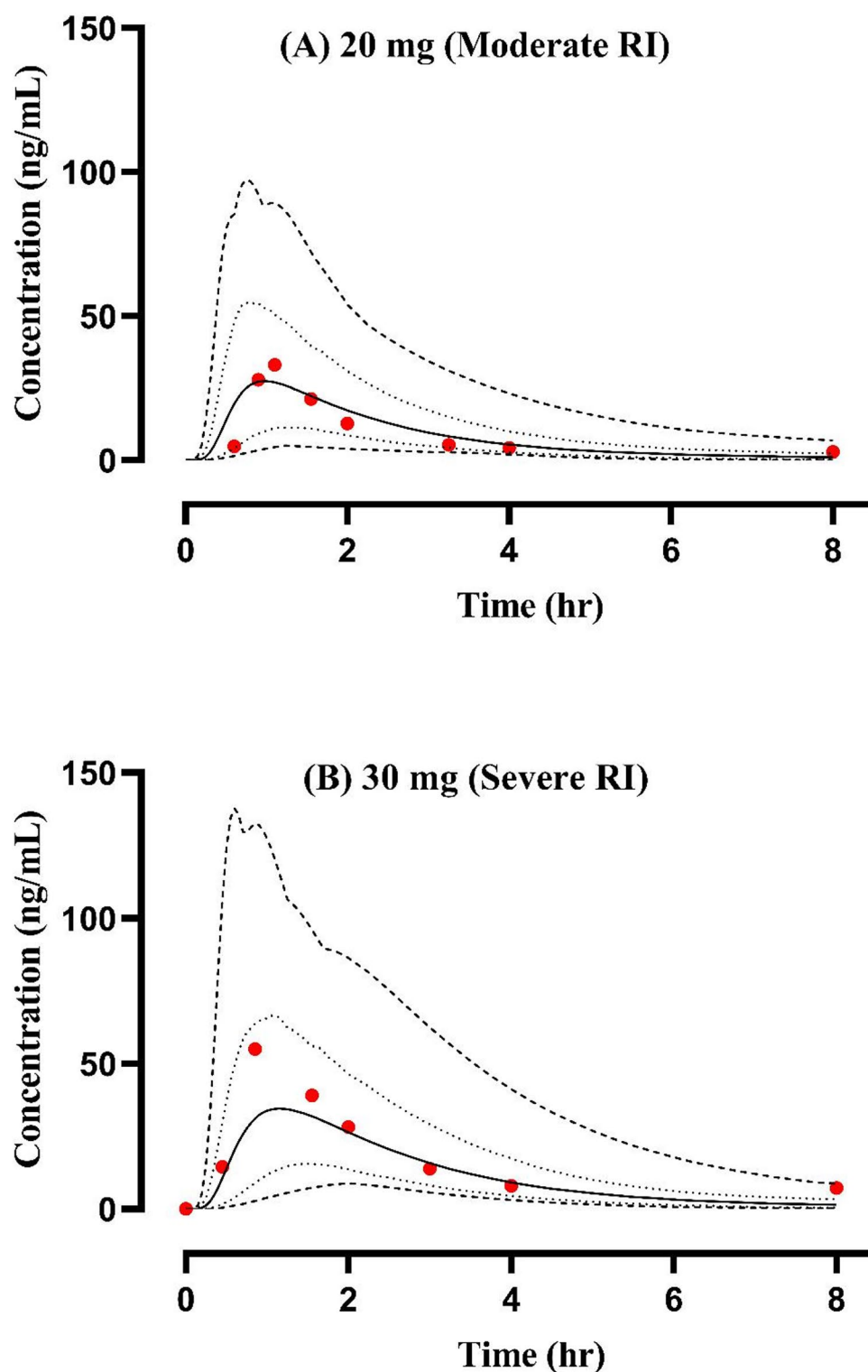


Fig. 6. The contrast of predicted and observed concentration–time curves following oral administration of nicardipine in renal impairment (RI) patients at dosages of (A) 20 mg⁴¹ (Moderate RI), (B) 30 mg⁴¹ (Severe RI), respectively. (Red dots): Values of observed data, (straight line): Arithmetic mean prediction, (dashed line): dashed lines–maximum and minimum values, (dotted line): dotted lines–5th and 95th percentile.

Conclusion

The developed PBPK model has successfully anticipated the ADME of nicardipine in healthy, cirrhotic, and renal impairment populations following oral and IV dosing. This model has been refined to yield more accurate predictions by integrating various pathophysiological factors associated with LC and CKD, thus providing

PK variables	AFE
IV healthy	
C_{max} (ng/mL)	0.896
$AUC_{0-\infty}$ (ng.h/mL)	0.951
CL (L/h)	1.059
Oral healthy	
C_{max} (ng/mL)	1.167
$AUC_{0-\infty}$ (ng.h/mL)	1.089
CL/F (L/h)	0.945
Renal failure	
C_{max} (ng/mL)	0.702
$AUC_{0-\infty}$ (ng.h/mL)	0.776
CL/F (L/h)	1.322
Liver cirrhosis	
C_{max} (ng/mL)	1.109
$AUC_{0-\infty}$ (ng.h/mL)	0.563
CL/F (L/h)	1.775

Table 5. Calculation of the AFE values for PK variables among healthy and diseased populations. *PK* pharmacokinetics, $AUC_{0-\infty}$ area underneath the curve from time zero to infinity, C_{max} maximal plasma concentration, *CL* clearance, *AFE* average fold error.

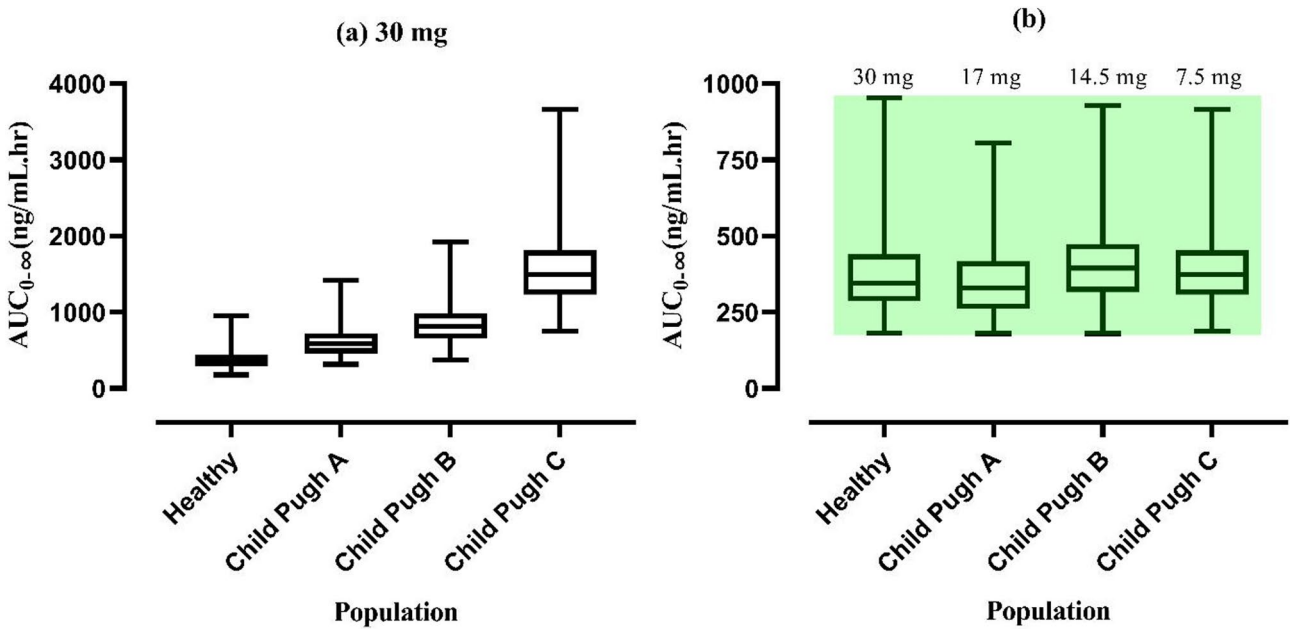


Fig. 7. Box plots illustrate the simulated $AUC_{0-\infty}$ with the 5th – 95th percentiles following a 30 mg oral dose of nicardipine in both healthy individuals and those with hepatic dysfunction (a). Suggested dosage reductions for patients with mild (CP-A), moderate (CP-B), and severe (CP-C) are presented in (b) for comparison with the exposure levels in healthy individuals. $AUC_{0-\infty}$ area underneath the curve from time zero to infinity.

recommendations to healthcare professionals in optimizing dosing strategies for patients with compromised hepatic and renal function. Moreover, the model is capable of forecasting the variations in PK among CKD and LC patients exhibiting various levels of severity, i.e. mild, moderate, and severe.

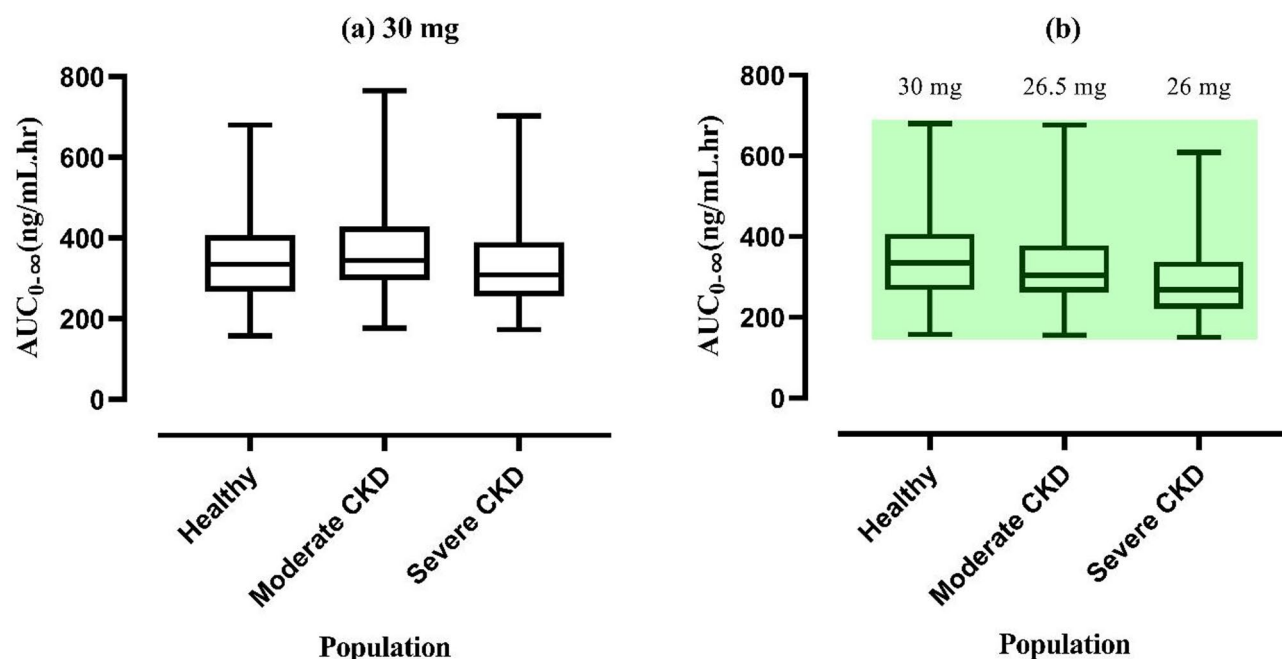


Fig. 8. Box plots illustrate the simulated $AUC_{0-\infty}$ with the 5th – 95th percentiles following a 30 mg oral dose of nicardipine in both healthy individuals and those with chronic kidney disease (CKD) (a). Suggested dosage reductions for patients with moderate and severe renal impairment are presented in (b) for comparison with the exposure levels in healthy individuals. $AUC_{0-\infty}$: area underneath the curve from time zero to infinity.

Data availability

All the data generated or evaluated during this study is reported in this manuscript.

Received: 17 December 2024; Accepted: 22 May 2025

Published online: 05 June 2025

References

- Baxter, L. T., Zhu, H., Mackensen, D. G., Butler, W. F. & Jain, R. K. Biodistribution of monoclonal antibodies: scale-up from mouse to human using a physiologically based Pharmacokinetic model. *Cancer Res.* **55**, 4611–4622 (1995).
- Baxter, L. T., Zhu, H., Mackensen, D. G. & Jain, R. K. Physiologically based Pharmacokinetic model for specific and nonspecific monoclonal antibodies and fragments in normal tissues and human tumor xenografts in nude mice. *Cancer Res.* **54**, 1517–1528 (1994).
- Lee, H. A., Leavens, T. L., Mason, S. E., Monteiro-Riviere, N. A. & Riviere, J. E. Comparison of quantum Dot biodistribution with a blood-flow-limited physiologically based Pharmacokinetic model. *Nano Lett.* **9**, 794–799 (2009).
- Theil, F. P., Guentert, T. W., Haddad, S. & Poulin, P. Utility of physiologically based Pharmacokinetic models to drug development and rational drug discovery candidate selection. *Toxicol. Lett.* **138**, 29–49 (2003).
- Rowland, M., Peck, C. & Tucker, G. Physiologically-based pharmacokinetics in drug development and regulatory science. *Annu. Rev. Pharmacol. Toxicol.* **51**, 45–73 (2011).
- Teorell, T. Kinetics of distribution of substances administered to the body, I: the extravascular modes of administration. *Arch. Int. Pharmacodyn. Ther.* **57**, 205–225 (1937).
- Clewell, R. A. & Clewell, I. I. Development and specification of physiologically based Pharmacokinetic models for use in risk assessment. *Regul. Toxicol. Pharmacol.* **50**, 129–143 (2008).
- Hartmanshenn, C., Scherholz, M. & Androulakis, I. P. Physiologically-based Pharmacokinetic models: approaches for enabling personalized medicine. *J. Pharmacokinet. Pharmacodyn.* **43**, 481–504 (2016).
- Peters, S. A. Evaluation of a generic physiologically based Pharmacokinetic model for lineshape analysis. *Clin. Pharmacokinet.* **47**, 261–275 (2008).
- Rasool, M. F. et al. Development and evaluation of physiologically based Pharmacokinetic drug-disease models for predicting Captopril Pharmacokinetics in chronic diseases. *Sci. Rep.* **11**, 8589 (2021).
- Zamir, A. et al. Physiologically based Pharmacokinetic model to predict Metoprolol disposition in healthy and disease populations. *ACS Omega*. **8**, 29302–29313 (2023).
- Adiuidjaja, J., Spire, J. & Brouwer, K. L. Physiologically based Pharmacokinetic (PBPK) model predictions of disease mediated changes in drug disposition in patients with nonalcoholic fatty liver disease (NAFLD). *Pharm. Res.* **41**, 441–462 (2024).
- Zhou, J. et al. Dosage adjustment for Ceftazidime in pediatric patients with renal impairment using physiologically based Pharmacokinetic modeling. *J. Pharm. Sci.* **110**, 1853–1862 (2021).
- Rasool, M. F., Khalil, F. & Läer, S. Optimizing the clinical use of carvedilol in liver cirrhosis using a physiologically based Pharmacokinetic modeling approach. *Eur. J. Drug Metab. Pharmacokinet.* **42**, 383–396 (2017).
- Pasha, M. et al. A comprehensive physiologically based Pharmacokinetic model for predicting vilaglipitin pharmacokinetics: insights into dosing in renal impairment. *Pharmaceuticals* **17**, 924 (2024).
- Jung, Y. H. et al. Effect of concomitant oral administration of ethanol on the pharmacokinetics of Nicardipine in rats. *Biomed. Chromatogr.* **36**, e5425 (2022).

17. Hofmann, F., Nastainczyk, W., Röhrkasten, A., Schneider, T. & Sieber, M. Regulation of the L-type calcium channel. *Trends Pharmacol. Sci.* **8**, 393–398 (1987).
18. Struyker-Boudier, H., Smits, J. & De Mey, J. The Pharmacology of calcium antagonists: a review. *J. Cardiovasc. Pharmacol.* **15**, S1–S10 (1990).
19. Bean, B. P. Two kinds of calcium channels in canine atrial cells. Differences in kinetics, selectivity, and Pharmacology. *J. Gen. Physiol.* **86**, 1–30 (1985).
20. Krishnaiah, Y., Satyanarayana, V. & Karthikeyan, R. Effect of the solvent system on the in vitro permeability of Nicardipine hydrochloride through excised rat epidermis. *J. Pharm. Pharm. Sci.* **5**, 123–130 (2002).
21. Ayub, A. et al. Clinical pharmacokinetics and pharmacodynamics of Nicardipine; a systematic review. *Expert Opin. Drug Metab. Toxicol.* **20**, 1053–1067 (2024).
22. Timour, G., Frédéric, V., Olivier, S. & Shango, D. N. Nicardipine-induced acute respiratory failure: case report and literature review. *Clin. Case Rep.* **11**, e7186 (2023).
23. Jun-Shik, C., Sung-Il, H. & Dong-Hyun, C. Effects of Atorvastatin on the pharmacokinetics of Nicardipine after oral and intravenous administration in rats. *Korean Soc. Appl. Pharmacol.* **18**, 226–232 (2010).
24. Nakamura, K. et al. Inhibitory effects of Nicardipine to cytochrome P450 (CYP) in human liver microsomes. *Biol. Pharm. Bull.* **28**, 882–885 (2005).
25. Dow, R. & Graham, D. A review of the human metabolism and pharmacokinetics of Nicardipine hydrochloride. *Br. J. Clin. Pharmacol.* **22**, 195S (1986).
26. Naud, J., Nolin, T. D., Leblond, F. A. & Pichette, V. Current Understanding of drug disposition in kidney disease. *J. Clin. Pharmacol.* **52**, 10S–22S (2012).
27. Drici, M. et al. Clinical Pharmacology of Nicardipine in liver transplant patients. *Fundam. Clin. Pharmacol.* **7**, 531–536 (1993).
28. Edginton, A. N. & Willmann, S. Physiology-based simulations of a pathological condition: prediction of pharmacokinetics in patients with liver cirrhosis. *Clin. Pharmacokinet.* **47**, 743–752 (2008).
29. Johnson, T. N., Boussery, K., Rowland-Yeo, K., Tucker, G. T. & Rostami-Hodjegan, A. A semi-mechanistic model to predict the effects of liver cirrhosis on drug clearance. *Clin. Pharmacokinet.* **49**, 189–206 (2010).
30. Rowland Yeo, K., Aarabi, M., Jamei, M. & Rostami-Hodjegan, A. Modeling and predicting drug pharmacokinetics in patients with renal impairment. *Expert Rev. Clin. Pharmacol.* **4**, 261–274 (2011).
31. Malik, P. R. et al. A physiological approach to pharmacokinetics in chronic kidney disease. *J. Clin. Pharmacol.* **60**, S52–S62 (2020).
32. Lee, J. M., Yoon, J. H., Maeng, H. J. & Kim, Y. C. Physiologically based Pharmacokinetic (PBPK) modeling to predict CYP3A-mediated drug interaction between saxagliptin and Nicardipine: bridging rat-to-human extrapolation. *Pharmaceutics* **16**, 280 (2024).
33. Campbell, B., Kelman, A. & Hillis, W. Noninvasive assessment of the haemodynamic effects of Nicardipine in normotensive subjects. *Br. J. Clin. Pharmacol.* **20**, 55S–61S (1985).
34. Graham, D. et al. The metabolism and pharmacokinetics of Nicardipine hydrochloride in man. *Br. J. Clin. Pharmacol.* **20**, 23S–28S (1985).
35. Wagner, J. G. et al. Single intravenous dose and steady-state oral dose pharmacokinetics of Nicardipine in healthy subjects. *Biopharm. Drug Dispos.* **8**, 133–148 (1987).
36. Hirota, N., Yonemaru, H., Yoshikawa, M., Naruto, H. Pharmacokinetics of Nicardipine following intravenous and oral administration to the same human subject. *Drug Metab. Pharmacokinet.* **13**, 376–381 (1998).
37. Rocha, P., Guerret, M., David, D., Marchand, X. & Kahn, J. Kinetics and hemodynamic effects of intravenous Nicardipine modified by previous propranolol oral treatment. *Cardiovasc. Drugs Ther.* **4**, 152S–153S (1990).
38. Modi, N. B., Veng-Pedersen, P., Graham, D. J. & Dow, R. J. Application of a system analysis approach to population pharmacokinetics and pharmacodynamics of Nicardipine hydrochloride in healthy males. *J. Pharm. Sci.* **82**, 705–713 (1993).
39. Razak, T. et al. The effect of hepatic cirrhosis on the pharmacokinetics and blood pressure response to Nicardipine. *Clin. Pharmacol. Ther.* **47**, 463–469 (1990).
40. Rosseel, M. & Lefebvre, R. Capillary gas chromatographic determination with nitrogen–phosphorus detection of the calcium antagonist Nicardipine and its pyridine metabolite M-5 in plasma. *J. Chromatogr. A* **668**, 475–480 (1994).
41. Lee, S. M., Williams, R., Warnock, D., Emmett, M. & Wollbach, R. A. The effects of Nicardipine in hypertensive subjects with impaired renal function. *Br. J. Clin. Pharmacol.* **22**, 297S (1986).
42. Yamane, N. et al. Microdose clinical trial: quantitative determination of Nicardipine and prediction of metabolites in human plasma. *Drug Metab. Pharmacokinet.* **24**, 389–403 (2009).
43. Willmann, S. et al. PK-Sim: a physiologically based Pharmacokinetic ‘whole-body’ model. *Biosilico* **1**, 121–124 (2003).
44. Amenta, F., Tomassoni, D., Traini, E., Mignini, F. & Veglio, F. Nicardipine: a hypotensive dihydropyridine-type calcium antagonist with a peculiar cerebrovascular profile. *Clin. Exp. Hypertens.* **30**, 808–826 (2008).
45. Budavari, S. The Merck index, Merck research laboratories, Merck and Co. Inc. *Whitehouse Stn. NJ*, 7401 (1996).
46. Urien, S., Albengres, E., Comte, A., Kiechel, J. R. & Tillement, J. P. Plasma protein binding and erythrocyte partitioning of Nicardipine in vitro. *J. Cardiovasc. Pharmacol.* **7**, 891–898 (1985).
47. PubChem Compound Summary for CID 4474, Nicardipine. *National Center for Biotechnology Information* (2024). (2024).
48. Li, C., Liu, T., Cui, X., Uss, A. S. & Cheng, K. C. Development of in vitro Pharmacokinetic screens using Caco-2, human hepatocyte, and Caco-2/human hepatocyte hybrid systems for the prediction of oral bioavailability in humans. *J. BioMol. Screen.* **12**, 1084–1091 (2007).
49. Holt, K., Ye, M., Nagar, S. & Korzekwa, K. Prediction of tissue-plasma partition coefficients using microsomal partitioning: incorporation into physiologically based Pharmacokinetic models and steady-state volume of distribution predictions. *Drug Metab. Dispos.* **47**, 1050–1060 (2019).
50. Beaumont, K., Gardner, I., Chapman, K., Hall, M. & Rowland, M. Toward an integrated human clearance prediction strategy that minimizes animal use. *J. Pharm. Sci.* **100**, 4518–4535 (2011).
51. Newman, E. M. & Rowland, A. A physiologically based Pharmacokinetic model to predict the impact of metabolic changes associated with metabolic associated fatty liver disease on drug exposure. *Int. J. Mol. Sci.* **23**, 11751 (2022).
52. Kalam, M. N. et al. Development and evaluation of a physiologically based Pharmacokinetic drug-disease model of propranolol for suggesting model informed dosing in liver cirrhosis patients. *Drug Des. Dev. Therapy*, 1195–1211 (2021).
53. Jing, J. *Pharmacokinetics and Physiologically Based Pharmacokinetic Modeling of Xenobiotic Disposition in Special Populations*, (2017).
54. George, N. et al. Chemistry and Pharmacological activities of Biginelli product-A brief overview. *Curr. Drug Discov. Technol.* **16**, 127–134 (2019).
55. Silva, C. F., Nascimento, C. S. Jr & Borges, K. Restricted dual access polypyrrole as an adsorbent in Pipette-Tip Solid-Phase extraction for simultaneous determination of nimodipine and Nicardipine from breast milk. *Available SSRN* **4236450** (2022).
56. Webster, A. C., Nagler, E. V., Morton, R. L. & Masson, P. Chronic kidney disease. *Lancet* **389**, 1238–1252 (2017).
57. Schuppan, D. & Afdhal, N. H. Liver cirrhosis. *Lancet* **371**, 838–851 (2008).
58. Rodighiero, V. Effects of liver disease on pharmacokinetics: an update. *Clin. Pharmacokinet.* **37**, 399–431 (1999).
59. Bergstrand, M., Hooker, A. C., Wallin, J. E. & Karlsson, M. O. Prediction-corrected visual predictive checks for diagnosing nonlinear mixed-effects models. *AAPS J.* **13**, 143–151 (2011).

60. Zhang, Y., Huo, M., Zhou, J., Xie, S. & PKSolver An add-in program for Pharmacokinetic and pharmacodynamic data analysis in Microsoft excel. *Comput. Methods Programs Biomed.* **99**, 306–314 (2010).
61. Franchetti, Y. & Nolin, T. D. Dose optimization in kidney disease: opportunities for PBPK modeling and simulation. *J. Clin. Pharmacol.* **60**, S36–S51 (2020).
62. Mignini, F. et al. Bioequivalence study of Nicardipine solution versus Nicardipine tablets. *Clin. Exp. Hypertens.* **26**, 375–386 (2004).
63. Heimbach, T. et al. Physiologically-based Pharmacokinetic modeling in renal and hepatic impairment populations: a pharmaceutical industry perspective. *Clin. Pharmacol. Ther.* **110**, 297–310 (2021).
64. Willmann, S. et al. Applications of physiologically based Pharmacokinetic modeling of rivaroxaban—Renal and hepatic impairment and drug-drug interaction potential. *J. Clin. Pharmacol.* **61**, 656–665 (2021).

Acknowledgements

The authors extend their appreciation to the King Salman Center for Disability Research for funding this work through Research group no KSRG-2024-433.

Author contributions

Conceptualization: A.A., M.F.R., F.A.; Methodology: A.A., A.Z., U.A.; Formal analysis and investigation: A.A., A.Z., U.A.; Writing—original draft preparation: A.A., A.Z., U.A.; Writing—review and editing: A.A., M.F.R., F.A.; Supervision: M.F.R., F.A. All authors have significantly contributed to the design, data extraction, analysis, and interpretation, and have participated in drafting and revising the manuscript. All the authors have agreed to submit the final version to the journal and accept responsibility for all aspects of the work.

Funding

King Salman Center for Disability Research Research group no KSRG-2024-433.

Declarations

Competing interests

The authors declare no competing interests.

Additional information

Supplementary Information The online version contains supplementary material available at <https://doi.org/10.1038/s41598-025-03829-4>.

Correspondence and requests for materials should be addressed to M.F.R. or F.A.

Reprints and permissions information is available at www.nature.com/reprints.

Publisher's note Springer Nature remains neutral with regard to jurisdictional claims in published maps and institutional affiliations.

Open Access This article is licensed under a Creative Commons Attribution-NonCommercial-NoDerivatives 4.0 International License, which permits any non-commercial use, sharing, distribution and reproduction in any medium or format, as long as you give appropriate credit to the original author(s) and the source, provide a link to the Creative Commons licence, and indicate if you modified the licensed material. You do not have permission under this licence to share adapted material derived from this article or parts of it. The images or other third party material in this article are included in the article's Creative Commons licence, unless indicated otherwise in a credit line to the material. If material is not included in the article's Creative Commons licence and your intended use is not permitted by statutory regulation or exceeds the permitted use, you will need to obtain permission directly from the copyright holder. To view a copy of this licence, visit <http://creativecommons.org/licenses/by-nc-nd/4.0/>.

© The Author(s) 2025